

Modal data-based simple statistical analysis as an effective petrogenetic indicator: a study from Kadavur gabbro-anorthosite complex, Tamil Nadu, southern India

Debaleena Sarkar, Jyotisankar Ray*, Papiya Banerjee and Suranjana Kayal

Department of Geology, University of Calcutta, 35, B.C. Road, Kolkata 700 019, India

Field and petrographic studies on the Neoproterozoic Kadavur intrusive complex (10°35'N, 78°11'E) (located in the Southern Granulite Terrane of the Indian shield) reveal three distinct types: (i) earliest phase of deformed schistose gabbro-anorthosite; (ii) most dominant layered gabbro-anorthosite, and (iii) locally developed pegmatoidal gabbro-anorthosite. A simple modal data-based statistical analysis of layered gabbro-anorthosite type yields highly significant or significant correlation coefficients for different mineralogical parameters and strongly supports differentiation from a common magma. Typical dispositions of the mineralogical parameters (as depicted by isopleths patterns) suggest maintenance of a magmatic lineage in varying hydration ambience that developed several petrographic variants within the layered type.

Keywords: Gabbro-anorthosite, isopleths map, mineralogical parameters, modal data, statistical analysis.

MODAL analysis studies on gabbro-anorthosites have been useful to classify and characterize such rocks. For example, Ashwal¹ worked out the genesis of the Mount Marcy anorthosite massif (Adirondacks, New York, USA) with a particular focus on anorthositic rocks associated with the high-grade terrain^{2,3}. Even for the Apollo-11 samples, modal analyses helped ascertain the heterogeneity in the lunar highland series⁴. However, in recent times, such modal analysis-based approaches for gabbro-anorthosites are lacking. In reality, modal data of igneous rocks represent the actual mineralogical composition and help in accurate nomenclature. Nowadays, however, the emphasis has shifted to other domains, presumably because of the availability of major, trace and isotopic data^{5,6}. Even in this scenario, in the recent past, modal data-based studies have helped resolve the long-standing controversy related to the accretion of gabbroic lower crust at the ridge axis⁷. In this context of the intrusive gabbro-anorthosite complex near Kadavur (10°35'N, 78°11'E), southern India (Figure 1), the present study performs statistical analyses of several mineralogical parameters to present a cogent petrogenetic history. The Kadavur complex was initially reported

from the Southern Granulite Terrane (SGT) of the Indian shield (Figure 1 a)^{8,9}. However, during 1980s, the region (hosting the Kadavur complex) was known as the Eastern Ghats Belt¹⁰. Early studies on the Kadavur complex suggest that: (i) the intrusion represents a funnel-shaped concordant body and (ii) the complex bears geological similarities with the Adirondack mountains¹¹. However, later studies have argued against the similarities between the Kadavur complex and intrusive rocks in the Adirondack region¹²; on the contrary, it was compared with early Archean, layered gabbro-anorthosite complex. It has been suggested that the Kadavur complex manifests multiple phases of magmatism with corresponding mappable attributes^{13,14}. Recent workers suggest a tholeiitic parentage and an inferred age of ~810 Ma for the anorthositic intrusions^{15,16}. However, it is unclear whether the complex is a product of differentiation from common parent magma or corresponds to discrete and separate magmatic pulses. Hence, this study attempts to resolve this issue with the help of statistical analyses of modal data and relevant correlation characteristics amongst mineralogical parameters.

The present work involves field studies, petrographic analyses and detailed statistical studies on modal variables that help throw light on the petrogenesis of the Kadavur

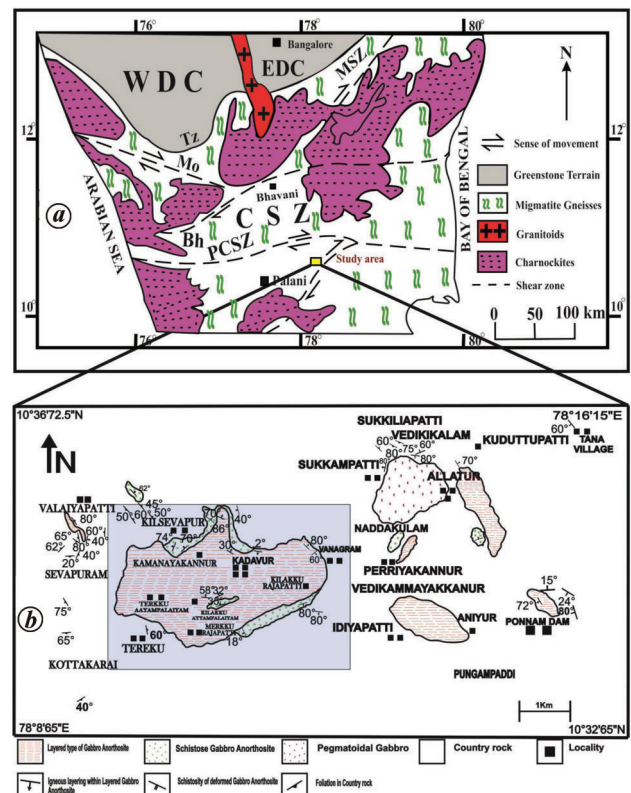


Figure 1. a, Location of the study area (Kadavur complex) within the regional tectonic frame of the Southern Granulite Terrane⁹. The complex falls within the branch-out portions of the Palghat-Cauvery shear zone⁵. b, Geological map of the Kadavur complex (by the present authors). Shaded portion represents the area where isopleths maps for different mineralogical parameters were constructed.

*For correspondence. (e-mail: jsray65@hotmail.com)

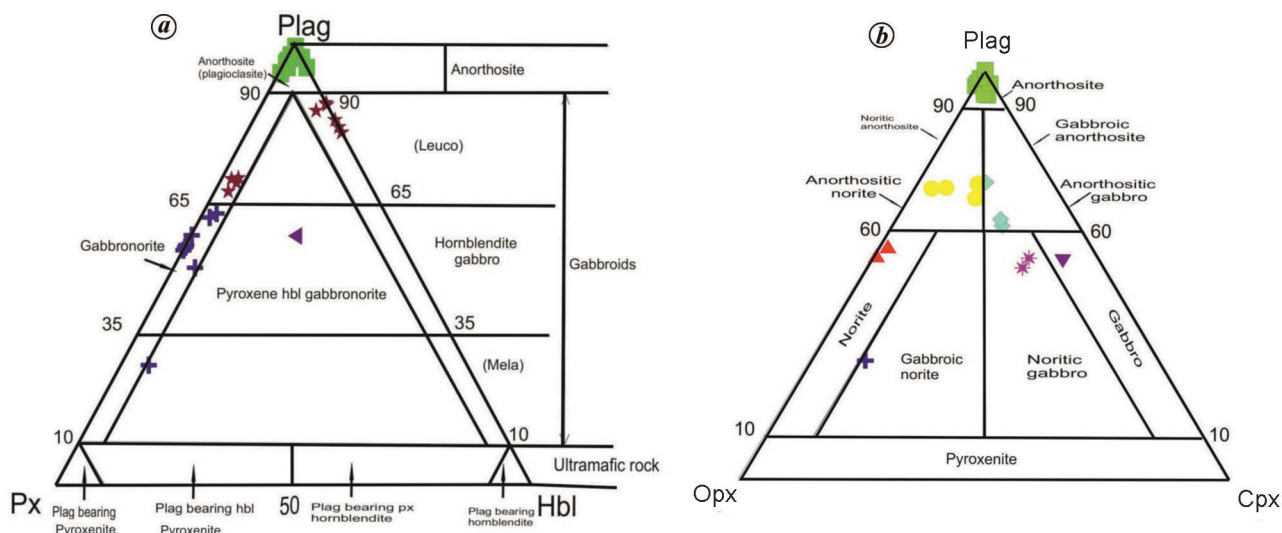


Figure 2 a, b. Plagioclase–pyroxene–hornblende and plagioclase–orthopyroxene–clinopyroxene mode-based triangular diagram for classification¹⁸.

complex. The complex is accommodated within country rocks which include hornblende schist, amphibolite, granite gneiss, quartzite and migmatite. The country rocks are often foliated with down-dip lineations. Some representative field photographs of the country rocks are provided in [Supplementary Figure 1](#). Field mapping indicates the presence of three distinct types of gabbro-anorthosite in the complex: (i) schistose gabbro-anorthosite; (ii) layered gabbro-anorthosite, and (iii) locally present pegmatoidal gabbro-anorthosite (Figure 1 b). Representative field photographs are given in [Supplementary Figures 2 and 3](#). Structural analyses often play an important role to understand the style of deformation in a terrane showing multiple folding and deformation. In this study, stereo pole diagrams of the foliation planes of country rocks have been constructed ([Supplementary Figure 4 a–c and e](#)), which indicate that the sheath fold geometry caused by a superposed pattern ([Supplementary Figure 4 d](#)) is being guided by the shearing mechanism¹⁷. The stereo pole diagram for the igneous foliation (developed on the layered gabbro-anorthosite-type) suggests evidence of intrusion with a nearly sub-vertical girdle axis ([Supplementary Figure 4 f](#)). In order to give an idea to the readers about the different types of intrusives within the Kadavur complex, representative hand-specimen photographs and photomicrographs have been furnished in [Supplementary Figure 5](#). Modal mineralogy (vol%) of the layered gabbro-anorthosite has been presented in [Supplementary Table 1](#) and projected on Plag–Px–Hbl (Figure 2 a) and Plag–Opx–Cpx (Figure 2 b) ternary diagrams following the IUGS recommendations¹⁸. It is apparent from Figure 2 a and b that there are several petrographic variants (so far as the nomenclature is concerned), and the corresponding IUGS-recommended names for each of the specimens have been tabulated in [Supplementary Table 1](#). Statistical studies based on modal-data variables of granitic rocks (and other

coarse-grained igneous rocks) to understand petrogenesis have been done by earlier workers^{19–24}. In addition, appropriate log-transformations need to be made on the modal data to eradicate the closure effect while calculating the correlation coefficients. In the present study, a total of 34 representative samples of layered gabbro-anorthosite were chosen to evaluate: (i) the average variation in mineralogical composition and (ii) the nature of correlation among the significant mineralogical parameters. For this, we collected point-count data using an automated point-counting stage mounted on a routine polarizing microscope²⁵. During modal data analysis, the following cautions were taken: (i) each slide was thoroughly examined immediately before the modal analysis so that the minerals could be identified easily and (ii) the number of point counts was kept sufficiently large (2000–2200) with a horizontal spacing of 0.3 mm and vertical spacing of 1 mm. For modal analysis, samples were chosen from different parts of the layered gabbro-anorthosite bodies on a half kilometre grid. Table 1 presents the arithmetic mean (\bar{X}), standard deviation, variance, skewness and kurtosis of different mineralogical parameters (log-normalized).

Six types of mineralogical parameters were chosen for correlation studies. These include anorthite percentage (An%) of plagioclase, colour index (CI), hydration index (HI), reciprocal of plagioclase crystallization index (RPCI), mafic crystallization index (MCI) and rock crystallization index (RCI) (Table 1). Percentage values of different data were transformed to Y using the transformation equation $Y = \log(X/100 - X)$, where X represents the present data, including several mineralogical parameters^{22,23}. CI was determined following the method given in the IUGS classification¹⁸. The other indices, namely HI, RPCI, MCI, RCI and An% of plagioclase, were also transformed using the same formula, i.e. $\log(X/100 - X)$. For easy comprehension, Table 1 gives explanations for the different indices.

Table 1. Statistical data for different mineralogical parameters[#]

Mineralogical parameters	Explanation*	Arithmetic mean (\bar{X})	Standard deviation	Variance	Kurtosis	Skewness
An% of plagioclase	–	0.21	0.12	0.014	0.0003	0.0005
Colour index (CI)	After IUGS ¹⁸	–0.85	0.54	0.29	0.17	–0.0074
Hydration index (HI)	Hbl + Biot	–3.29	0.68	0.46	0.45	–0.09
Reciprocal of plagioclase crystallization index (RPCI)	Plag	–3.44	0.8	0.64	0.65	–0.06
	Opq					
Mafic crystallization index (MCI)	Plag	–2.76	0.70	0.49	1.03	0.31
	Opq					
Rock crystallization index (RCI)	Hbl + Pyx + Biot	–1.06	0.97	0.95	3.29	0.33
	Hbl + Pyx + Biot + Epi + Apat					
	Opq					

*CI, HI, RPCI, MCI and RCI values were calculated on the basis of modal data (Supplementary Table 1).

Plag, Plagioclase; Hbl, Hornblende; Pyx, Pyroxene; Biot, Biotite; Apat, Apatite; Opq, Opaque; Epi, Epidote.

[#]Mineralogical parameters were log-normalized.

Table 2. Different mineralogical parameters and their respective correlation coefficients after normalized transformation

Pair of mineralogical parameters	Linear correlation coefficient (r)	Remark
RCI versus HI	0.42	Highly significant
HI versus CI	0.39	Significant
RPCI versus CI	0.8	Highly significant
MCI versus HI	–0.45	Highly significant
CI versus An% of plagioclase	–0.85	Highly significant
RPCI versus An% of plagioclase	–0.77	Highly significant

Degrees of freedom (F) = 32. Correlation coefficient values (at $F = 32$) were tested at 5% level of significance: 0.325 and at 1% level of significance: 0.418. Correlation coefficients greater than 0.418 are classified as highly significant whereas those ranging between 0.325 and 0.418 are classified as significant²⁶.

The significance of the calculated correlation coefficients (r) was tested at 5% and 1% levels of significance²⁶. Table 2 gives the linear correlation coefficient values. To understand the style of several spatial variations of the mineralogical parameters in the layered gabbro-anorthosite bodies, these attributes were plotted in isopleth maps (Figure 3 a–e). The RCI value showed a systematic decrease from the margin of the complex to its central part (Figure 3 a). These decreasing values are consistent with the low proportion of mafic minerals towards the centre, where the anorthositic band is most dominant (Figure 1 b). CI also showed a systematic decreasing pattern from the margin inwards (Figure 3 b). This observation attests to the presence of (plagioclase-dominant) anorthosite occurrence towards the centre. In concordance with the geological map (Figure 1 b), HI showed a gradual fall towards the central part of the complex dominated by an anorthosite layer (which crystallized under a relatively dry condition in the magma chamber) (Figure 3 c)²⁷. MCI (which depends on the reciprocal of hornblende, pyroxene and biotite modal data) showed a systematic decrease towards the peripheral part, which is consistent with the presence of mafic mineral-bearing gabbroic layers (Figure 3 d). Figure 3 e shows that RPCI decreases from the margin inwards. This reflects

a higher modal plagioclase percentage towards the (~anorthositic) central part. In Figure 3 a–e relevant threshold values have been given to track the style of differentiation readily.

Spatial variations of all the mineralogical parameters corroborate crystallization from initial anhydrous mafic magma. It is possible that for the Kadavur complex, crystallization of constituent minerals had been continuing in the magma chamber for a prolonged period following a similar process as documented for gabbro-anorthosite bodies from Kuliana region, Singhbhum, eastern India²⁴. The origin of Precambrian gabbro-anorthosite bodies has been variously interpreted as either invoking differentiation from a single magmatic lineage or as an outcome of several magmatic pulses. These are several proponents of a single magmatic differentiation history^{28–32}. According to Weaver *et al.*²⁸, the presence of hydrous phase (caused during melting of the depleted mantle) and crystal fractionation involving plagioclase cumulates play important roles in generating the gabbro-anorthosite (layered) complex. On the contrary, the multiple-stage model of development of gabbro-anorthosite mass has been invoked by a number of workers^{33–36}. Therefore, in the backdrop of the available petrogenetic analyses, it will be worthwhile to resolve

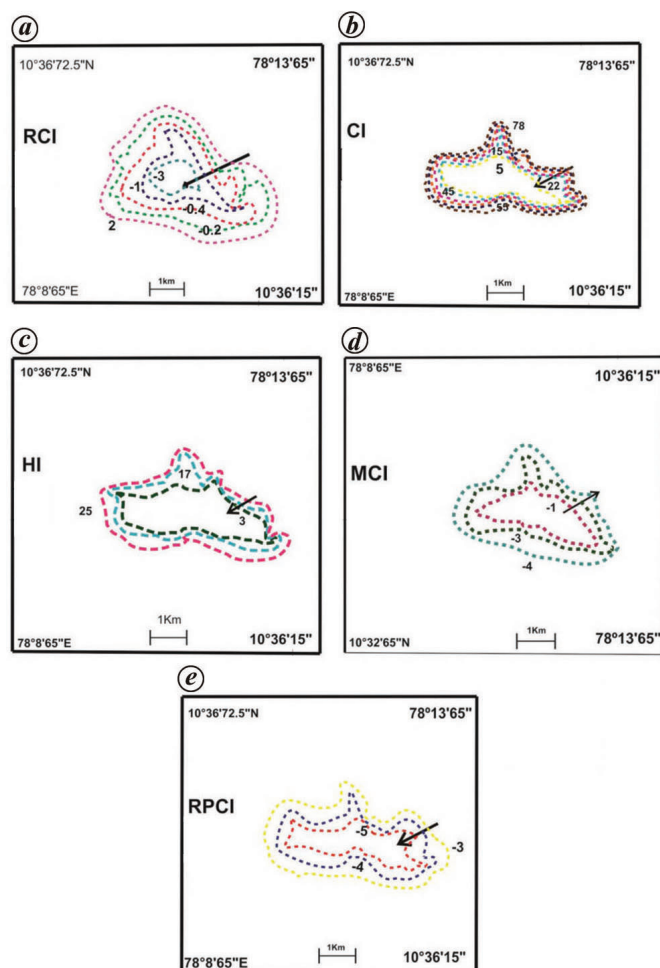


Figure 3. Isopleth maps for several mineralogical parameters within the spatial disposition of layered gabbro-anorthosite bodies (taken from Figure 1 *b* of the study area). In all cases arrowheads indicate progressively decreasing values of mineralogical parameters. Numerals represent relevant values of the contours (for details, see text). Explanations of mineralogical parameters are given in Table 1. Threshold values are as follows: *a*, RCI (rock crystallization index): (-3) for anorthosite > (-3) for gabbroic rocks; *b*, CI (colour index): <5 for anorthosite and >5 for gabbroic rocks; *c*, HI (hydration index): <3 for anorthosite and >3 for gabbroic rocks; *d*, MCI (mafic crystallization index): -1 for anorthosite and >(-1) for gabbroic rocks; *e*, RPCI (reciprocal of plagioclase crystallization): (-5) for anorthosite and >(-5) for gabbroic rocks.

this issue (single magmatic lineage or several magmatic pulses) for the present case.

Based on our simple statistical analyses of modal data of the Kadavur gabbro-anorthosite complex, we conclude the following important points:

- (1) The rocks in this complex represent a single magmatic lineage.
- (2) These rocks lack mineralogical records of mixing of different pulses of magma, at least during crystallization, if not during the pre-crystallization stage. On this basis, the rocks are interpreted to record the differentiation of a single magma of tholeiitic nature. The trend (and nature) of the differentiation process is well outlined by the appearance (or disappearance) of minerals (including hydrous phases) from the core to the periphery of the Kadavur complex.

1. Ashwal, L. D., Mineralogy of mafic and Fe-Ti oxide rich differentiates of the Marcy Anorthosite massif, Adirondacks, New York. *Am. Mineral.*, 1982, **67**, 14–27.
2. Singhinolfi, G. P. and Gorgoni, C., Genesis of massif-type anorthosites – the role of high grade metamorphism. *Contrib. Mineral. Petrol.*, 1975, **51**, 119–126.
3. Crosby, P., Petrogenetic and statistical implications of modal studies in Adirondack anorthosite. In *Origin of Anorthosite and Related Rocks* (ed. Isachsen, Y. W.), New York State Museum and Science Service Memoir, 1969, vol. 18, pp. 289–303.
4. Taylor, G. J., The composition of the lunar highlands: evidence from modal and normative plagioclase contents in anorthositic lithic fragments and glasses. *Earth Planet. Sci. Lett.*, 1972, **16**, 263–268.
5. Neymark, L. A., Amelin, V. Y. and Larrin, A. M., Pb–Nd–Sr isotopic and geochemical constraints on the origin of the 1.54–1.56 Ga Salmi Rapakivi Granite–Anorthosite Batholith (Karelia Russia). *Mineral. Petrol.*, 1994, **50**, 173–193.
6. Ram Mohan, M., Satyanarayanan, M., Santosh, M., Sylvester, P. J., Tubrett, M. and Rebecca, L., Neoproterozoic suprasubduction zone arc

- magmatism in southern India: Geochemistry, zircon U–Pb geochronology and Hf isotopes of the Sittampundi Anorthosite Complex. *Gondwana Res.*, 2013, **23**, 539–557.
7. Van Tongeren, J. A., Hirth, G. and Kelemen, P. B., Constraints on the accretion of the gabbroic lower oceanic crust from plagioclase lattice preferred orientation in the Samail ophiolites. *Earth Planet. Sci. Lett.*, 2015, **427**, 249–261.
 8. Chetty, T. R. K. and Rao, Y. J. B., The Cauvery Shear Zone, Southern Granulite Terrain, India: a crustal-scale flower structure. *Gondwana Res.*, 2006, **10**, 77–85.
 9. Santosh, M., The Southern Granulite Terrane: a synopsis. *Episodes*, 2020, **43**, 109–123.
 10. Subhramanyam, C. and Verma, R. K., Gravity field, structure and tectonics of Eastern Ghats. *Tectonophysics*, 1986, **126**, 195–212.
 11. Subramanian, A. P., Petrology of the anorthosite–gabbro mass at Kadavur, Madras, India. *Geol. Mag.*, 1956, **93**, 287–300.
 12. Windley, B. F. and Selvan, T. A., Anorthosites and associated rocks of Tamil Nadu, Southern India. *J. Geol. Soc. India*, 1975, **16**, 209–215.
 13. Sarkar, A. and Bose, M. K., Observations on the Kadavur igneous complex, Tiruchirappalli, Tamil Nadu. *India J. Earth Sci.*, 1978, **15**, 194–199.
 14. Sarkar, A. and Bose, M. K., Geology of the Kadavur complex, Tamil Nadu. *Rec. Res. Geol.*, 1987, **13**, 97–107.
 15. Kumar, V. M., Kumar, R. S., Rajaprian, K. and Singh, K., Petrography and major geochemical studies of anorthosite, Kadavur and adjoining area, Tamil Nadu, India. *Int. Res. J. Earth Sci.*, 2013, **1**, 15–22.
 16. Kooijman, E., Upadhyay, D., Mezger, K., Raith, M. M., Berndt, J. and Srikantappa, C., Response of the U–Pb chronometer and trace elements in zircon to ultrahigh-temperature metamorphism: the Kadavur anorthosite complex, southern India. *Chem. Geol.*, 2011, **290**, 177–188.
 17. Skjerna, L., Tubular folds and sheath folds: definitions and conceptual models for their development, with examples from Grapesvare area, northern Sweden. *J. Struct. Geol.*, 1989, **11**, 689–703.
 18. Streckeisen, A., To each plutonic rock its proper name. *Earth Sci. Rev.*, 1976, **12**, 1–33.
 19. Chayes, F., Numerological correlation and petrographic variation. *J. Geol.*, 1962, **70**, 440–452.
 20. Chayes, F., Effect of a single non zero open covariance on the simple closure test. In *Geostatistics* (ed. Merriam, D.), Plenum Press, New York, USA, 1970, pp. 11–22.
 21. Saha, A. K., Bhattacharya, C. and Lakshminpathy, S., Some problems of interpreting the correlation between the modal variables in granitic rocks. *J. Int. Assoc. Math. Geol.*, 1974, **6**, 245–258.
 22. Dasgupta, S., Ray, J., Mazumder, A., Sarkar, N. K., Das, S. and Dasgupta C., Correlation characteristics among mineralogical parameters in Porphyritic granite bodies around Raghunathpur, Purulia district, West Bengal. *J. Geol. Soc. India*, 2000, **54**, 263–270.
 23. Hazra, S., Saha, P., Ray J. and Podder, A., Simple statistical and mineralogical studies as petrogenetic indicator for Neoproterozoic Myllem porphyritic granites of East Khasi hills, Meghalaya, North eastern India. *J. Geol. Soc. India*, 2010, **75**, 760–768.
 24. Chakraborti, T. M., Ray, A. and Deb, G. K., Crystal size distribution analysis of plagioclase from gabbro-anorthosite suite of Kuli-ana, Orissa, eastern India: implication for textural coarsening in a static magma chamber. *Geol. J.*, 2015, **52**, 234–248.
 25. Chayes, F., A simple point counter for thin section. *Am. Mineral.*, 1949, **34**, 1–11.
 26. Snedecor, G. W. and Cochran, W. G., *Statistical Methods*, Oxford and IBH Publication, 1967, p. 593.
 27. Ashwal, L. D., *Anorthosites*, Springer-Verlag, Berlin, Germany, 1993, p. 422.
 28. Weaver, B. L., Tarney, J. and Windley, B., Geochemistry and petrogenesis of the Fiskenaeset anorthosite complex, southern West Greenland: nature of the parent magma. *Geochim. Cosmochim. Acta*, 1981, **45**(5), 711–725.
 29. Girardi, V. A. G., Rivalenti, G. and Sinigoi, S., The petrogenesis of the Niquelandia layered, basic–ultrabasic complex, Central Goias, Brazil. *J. Petrol.*, 1986, **27**, 715–744.
 30. Polat, A., Brian, J. F., Peter, W. U. A., Kalvig, P., Kerrich, R., Dilek, Y. and Yang, Z., Geochemistry of anorthositic differentiated sills in the Archean (~2970 Ma) Fiskenaeset Complex, SW Greenland: implications for parental magma compositions, geodynamic setting, and secular heat flow in arcs. *Lithos*, 2011, **123**, 50–72.
 31. Berger, J. *et al.*, Petrogenesis of Archean PGM bearing chromitites and associated ultramafic–mafic–anorthositic rocks from the Guelb el Azib layered complex (West African craton, Mauritania). *Precambrian Res.*, 2013, **224**, 612–628.
 32. Pinto, V. M. *et al.*, Petrogenesis of the mafic–ultramafic Canindé layered intrusion, Sergipano Belt, Brazil: constraints on the metallogenesis of the associated Fe–Ti oxide ores. *Ore Geol. Rev.*, 2020; <https://doi.org/10.1016/j.oregeorev.2020.103535>.
 33. Longhi, J. and Ashwal, L. D., Two-stage models for lunar and terrestrial anorthosites: petrogenesis without a magma ocean. *J. Geophys. Res.*, 1985, **90**(2), C571–C584.
 34. Scoates, J. S. and Frost, C. D., A strontium and neodymium isotopic investigation of the Laramie anorthosites, Wyoming, USA: implications for magma chamber processes and the evolution of magma conduits in Proterozoic anorthosites. *Geochim. Cosmochim. Acta*, 1996, **60**(1), 95–107.
 35. Huang, H., Polat, A., Fryer, B. J., Peter, W. U. A. and Windley, B. F., Geochemistry of the Mesoarchean Fiskenaeset Complex at Majorqap qáva, SW Greenland: evidence for two different magma compositions. *Chem. Geol.*, 2012, **314–317**, 66–82.
 36. Bybee, G. M. *et al.*, Proterozoic massif-type anorthosites as the archetypes of long-lived (≥ 100 Myr) magmatic systems – new evidence from the Kunene Anorthosite Complex (Angola). *Precambrian Res.*, 2019; <https://doi.org/10.1016/j.precamres.2019.105393>.

ACKNOWLEDGEMENTS. We thank the University of Calcutta, Kolkata for funds (UGC-UPE II program) to carry out this study. We also thank two anonymous reviewers for their useful suggestions that helped improve the manuscript.

Received 29 July 2021; re-revised accepted 30 June 2022

doi: 10.18520/cs/v123/i4/601-605